Characterization of the Propionyl-CoA Synthetase (PrpE) Enzyme of *Salmonella enterica*: Residue Lys592 Is Required for Propionyl-AMP Synthesis†

Alexander R. Horswill and Jorge C. Escalante-Semerena*

Department of Bacteriology, University of Wisconsin-Madison, Madison, Wisconsin 53706

Received August 6, 2001; Revised Manuscript Received November 6, 2001

ABSTRACT: The propionyl-CoA synthetase (PrpE) enzyme of *Salmonella enterica* catalyzes the first step of propionate catabolism, i.e., the activation of propionate to propionyl-CoA. The PrpE enzyme was purified, and its kinetic properties were determined. Evidence is presented that the conversion of propionate to propionyl-CoA proceeds via a propionyl-AMP intermediate. Kinetic experiments demonstrated that propionate was the preferred acyl substrate ($k_{cat}/K_m = 1644\ mM^{-1}\ s^{-1}$). Adenosine 5′-propyl phosphate was a potent inhibitor of the enzyme, and inhibition kinetics identified a Bi Uni Uni Bi Ping Pong mechanism for the reaction catalyzed by the PrpE enzyme. Site-directed mutagenesis was used to change the primary sequence of the wild-type protein at positions G245A, P247A, K248A, K248E, G249A, K592A, and K592E. Mutant PrpE proteins were purified, and the effects of the mutations on enzyme activity were investigated. Both PrpEK592 mutant proteins (K592A and K592E) failed to convert propionate to propionyl-CoA, and plasmids containing these alleles of *prpE* failed to restore growth on propionate of *S. enterica* carrying null *prpE* alleles on their chromosome. Both PrpEK592 mutant proteins converted propionyl-AMP to propionyl-CoA, suggesting residue K592 played no discernible role in thioester bond formation. To the best of our knowledge, these mutant proteins are the first acyl-CoA synthetases reported that are defective in adenylation activity.

In *Salmonella enterica*, propionate is activated to propionyl-CoA by an acyl-CoA synthetase encoded by the *prpE* gene. This gene is part of the *prp* locus, *prpRBCDE*, which is required to catalyze steps of the 2-methylcitric acid cycle for propionate catabolism (*1*, *2*). The PrpE protein is required for growth of *S. enterica* on propionate and can substitute for the acetyl-CoA synthetase (Acs) enzyme during growth on acetate. Initial biochemical characterization of PrpE suggested the enzyme was an acyl-CoA synthetase capable of catalyzing propionyl-CoA or acetyl-CoA formation (*3*). However, the kinetic properties of PrpE were not determined, and the role of conserved residues in this enzyme was not investigated.

Acyl-CoA synthetases, such as PrpE, are the primary route for fatty acid activation in organisms. These enzymes activate acyl groups in a two-step reaction mechanism, which proceeds through an acyl-adenylate (acyl-AMP) intermediate (Figure 1) (*4*, *5*). Acyl-CoA synthetases fall into a large group of enzymes that catalyze reactions through adenylated intermediates, called the acyl-adenylate/thioester forming family (*6*). This family of enzymes is similar at the amino acid and structural level, and includes enzymes as diverse as peptide synthetase adenylation domains, α-aminoadipate reductases, and luciferases (*7*). These enzymes have recently generated considerable interest due to their industrial and medical importance. For example, acyl-CoA synthetases have been used to incorporate unusual acyl groups into biopolymers and polyketide antibiotics (*8*−*10*), adenylation domains

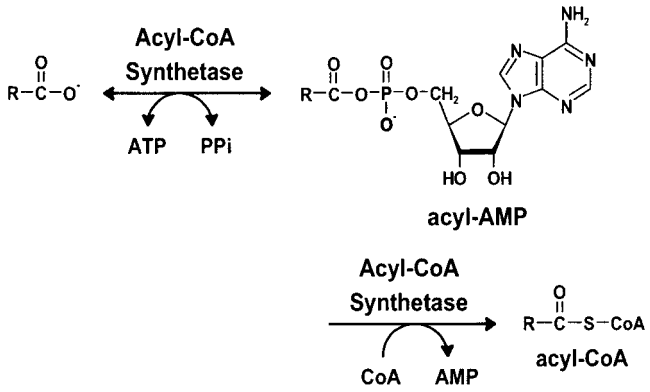

FIGURE 1: The acyl-CoA synthetase reaction. This reaction proceeds through an acyl-AMP intermediate. In the case of PrpE, the R group would be CH_3-CH_2- for propionate.

of peptide synthetases can be altered to generate novel peptide antibiotics (*11*), and luciferase is widely used as a reporter for ATP levels (*12*, *13*). Sequence similarity among members of this enzyme family is often very low (*6*), and candidates are usually identified by several conserved motifs (Figure 2).

Motif 1 is considered the signature motif of the acyl-adenylate/thioester forming enzymes and has been investigated in several members of this family. This motif is part of a flexible loop that is disordered in the crystal structures of *Photinus pyralis* luciferase and the L-phenylalanine adenylation domain of gramicidin S synthetase (PheA) of *Bacillus brevis* (*7*, *14*). The structure of PheA suggests motif 1 may be positioned for pyrophosphate release during adenylate formation (*7*). Initial site-directed mutagenesis experiments at this motif in *Bacillus brevis* tyrocidine synthetase (TycA) suggested that the conserved residues

* Corresponding author: Telephone: (608)262−7379; fax: (608)-262−9865; e-mail: escalante@bact.wisc.edu.

† This work was supported by NIH Grant GM62203. A.R.H. was supported by NIH biotechnology training grant GM08349 and a NSF predoctoral fellowship.

10.1021/bi015647q CCC: $22.00
Published on Web 01/19/2002

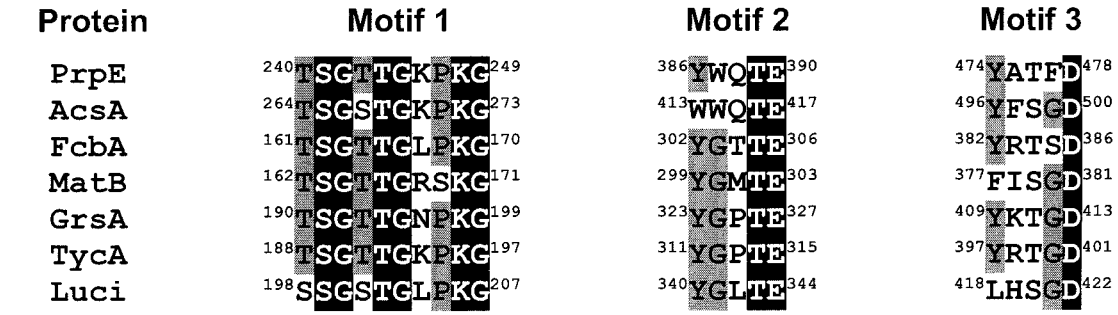

FIGURE 2: Conserved motifs in the adenylate/thioester-forming enzyme family. These motifs have been previously described (*17*). The abbreviations for the sequences are as follows: PrpE, *S. enterica* PrpE (*1*); Acs, *E. coli* acetyl-CoA synthetase (*44*); FcbA, *Pseudomonas* sp. DJ-12 4-chlorobenzoyl CoA synthetase (*6*); MatB, *R. trifolii* malonyl-CoA synthetase (*45*); GrsA, *Bacillus brevis* gramicidin synthetase (*46*); TycA, *B. brevis* tyrocidine synthetase 1 (*47*); Luci, *Photinus pyralis* luciferase (*48*).

might be important for catalysis (*15*), and further studies of the TycA enzyme indicated residue K186 of this motif (K248 of PrpE) may orient the β and γ phosphates of ATP during catalysis (*16*). Site-directed mutagenesis on the 4-chlorobenzoate (4-CBA) CoA synthetase of *Pseudomonas* strain CBS3, and NMR spectroscopy and modeling studies of malonyl-CoA synthetase of *Rhizobium trifolii* identified residues of motif 1 that were involved in acyl-AMP synthesis (*17*, *18*). These studies on adenylation domains and CoA synthetases suggested that motif 1 was involved in adenylate formation. However, the exact role of this motif in the enzyme mechanism and in vivo remains unclear.

Recently, studies on the role of residue K529 of luciferase (K592 of PrpE) showed that this residue was required for luciferyl-AMP formation and not the oxidation reaction to oxyluciferin (*19*). This report was the first identification of a residue that was specifically required for adenylate formation in the acyl-adenylate/thioester forming enzyme family. In the crystal structure of gramicidin S synthetase, the corresponding lysine residue (K517) forms electrostatic interactions with the phosphate of AMP and the carboxylate of L-phenylalanine, suggesting that this residue is also required for adenylation formation in peptide synthetases (*7*).

The interest in the adenylate/thioester-forming enzyme family has prompted numerous studies on their kinetic properties and function of conserved protein motifs in vitro. However, little effort has been applied to the functional analysis of mutant enzymes with modifications in these motifs in vivo. In this report, the propionyl-CoA synthetase (PrpE) of *S. enterica* was characterized, and the function of conserved residues was addressed in vitro and in vivo. Residue K592 of PrpE enzyme was required for adenylate formation and for growth of *S. enterica* on propionate.

EXPERIMENTAL PROCEDURES

Culture Media and Growth Conditions. All chemicals were purchased from Sigma Chemical Co. (St. Louis, MO) unless otherwise stated. A list of strains and plasmids used and their genotypes is provided in Table 1. *Escherichia coli* cultures were maintained Luria-Bertani (LB) broth. Antibiotic concentrations in rich medium were (in μg/mL): ampicillin (Ap), 100; chloramphenicol (Cm), 50; kanamycin (Km), 50.

For the overexpression of PrpE proteins, overnight cultures of *E. coli* ER2566 strains were grown in 25 mL of LB broth containing Ap at 30 °C (*20*). Twenty milliliters of the overnight culture was inoculated into 1 L of SOC medium in a 2-L Erlenmeyer flask (*21*), which was incubated with shaking at 18−20 °C water bath. The culture was grown to an OD_{600} = 0.20−0.25, and protein overexpression was induced with IPTG (0.5 mM final concentration). After induction, the culture was incubated for an additional 16−18 h before cells were harvested.

Assessment of the Effect of Mutations in prpE during Growth on Propionate. No−Carbon E (NCE) medium was used as a minimal medium (*22*). *S. enterica* strains were grown overnight in LB broth, and the cultures were diluted 1:50 (vol/vol) into 5 mL of NCE medium supplemented with 1 mM $MgSO_4$, 0.5 mM methionine, 30 mM propionate, 50 μg/mL ampicillin, and trace minerals (*23*). Cultures were grown in 18 × 150 mm tubes, and growth was monitored at 650 nM using a Spectronic 20D spectrophotometer furnished with a red filter (Milton Roy, Rochester, NY).

Recombinant DNA and Genetic Techniques. Restriction and modification enzymes were purchased from Promega Corporation (Madison, WI) unless otherwise stated, and were used according to manufacturer's instructions. All DNA manipulations were performed in *E. coli* DH5α/F′. Plasmids were transformed into *E. coli* by $CaCl_2$ heat-shock as described (*21*). Plasmids were transformed into *S. enterica* by electroporation as described (*24*). Nonradioactive sequencing of plasmids was performed at the Biotechnology Center at the University of Wisconsin-Madison.

Plasmid Constructions. In all cases, the presence of mutations was verified by nucleotide sequencing.

Plasmids pPRP69, pPRP87−90. Site-directed mutations in motif 1 were created using mutagenic primers 5′ containing the *Aat*II site in *prpE*. The G245A mutation was PCR amplified using a 3′ mutagenic primer (5′-CCGCCGACGTCGCGCTGGACGCCTTTCGGTTTGGCGGT-3′) and a 5′ primer (5′-CATAGCCGTCCACCGTTTGCCC-3′). PCR was performed using conditions as described elsewhere (*25*). The 0.6-kb PCR products were purified using QIAquick PCR Purification kit, digested with *Aat*II and *SalI*, and cloned into pPRP68 digested with the same enzymes. The resulting plasmid was 9.4 kb (Ap^r) and was named pPRP69. To construct other site-directed mutations at this motif, the following

[1] Abbreviations: Ap, ampicillin; Cm, chloramphenicol; CoA, coenzyme A; D_2O, deuterated water; ESI-MS, electrospray ionization mass spectrometry; G6PDH, glucose-6-phosphate dehydrogenase; GSH, glutathione; HK, hexokinase; LDH, lactate dehydrogenase; Km, kanamycin; MK, myokinase; NMR, nuclear magnetic resonance; PEP, phosphoenolpyruvate; PK, pyruvate kinase; PMSF, phenylmethanesulfonyl fluoride; TBAB, tetrabutylammonium bromide; TCEP−HCl, Tris(2-carboxyethyl)phosphine hydrochloride.

Table 1: Strain List

strain or plasmid	genotype	reference or source[a]
	E. coli	
DH5α/F′	F′/*endA1 hsdR17* (r_k^- m_k^+) *supE44 thi-1 recA1 gyrA* (Na1^r) *relA1* Δ(*lacZYA-argF*)*U169 deoR* [*ϕ*80d*lac*Δ(*lacZ*)*M15*]	New England Biolabs
ER2566	F$^-$ *λ*$^-$ *fhuA2* [*lon*] *ompT lacZ::T7 geneI gal sulA11* Δ(*mcrC-mrr*)*114::IS10 R(mcr-73*::miniTn*10*)*2 R(zgb-210*::Tn*10*)*1* (Tet^s) *endA1 [dcm]*	New England Biolabs
JE4034	DH5α/pPRP37 (*prpE*$^+$, *cat*$^+$)	*1*
JE4153	DH5α/pPRP45 (*prpE*$^+$, *bla*+)	this study
JE4528	ER2566/pPRP45 (*prpE*$^+$, *bla*+)	this study
JE4298	DH5α/pPRP54 (*prpE*$^+$, *bla*+)	*3*
JE4813	ER2566/pPRP68 (T7 *rpo*$^+$, *prpE*$^+$, *bla*$^+$)	this study
JE5640	ER2566/pPRP69 (T7 *rpo*$^+$, *prpE*-G245A, *bla*$^+$)	this study
JE5641	ER2566/pPRP87 (T7 *rpo*$^+$, *prpE*-P247A, *bla*$^+$)	this study
JE5642	ER2566/pPRP88 (T7 *rpo*$^+$, *prpE*-K248A, *bla*$^+$)	this study
JE5643	ER2566/pPRP89 (T7 *rpo*$^+$, *prpE*-G249A, *bla*$^+$)	this study
JE5941	ER2566/pPRP90 (T7 *rpo*$^+$, *prpE*-K248E, *bla*$^+$)	this study
JE6182	ER2566/pPRP100 (T7 *rpo*$^+$, *prpE*-K592A, *bla*$^+$)	this study
JE6183	ER2566/pPRP101 (T7 *rpo*$^+$, *prpE*-K592E, *bla*$^+$)	this study
JE6270	DH5α/pPRP108 (P_{araBAD}, *prpE*$^+$, *bla*$^+$)	this study
JE6271	DH5α/pPRP109 (P_{araBAD}, *prpE*-G245A, *bla*$^+$)	this study
JE6272	DH5α/pPRP110 (P_{araBAD}, *prpE*-P247A, *bla*$^+$)	this study
JE6273	DH5α/pPRP111 (P_{araBAD}, *prpE*-K248A, *bla*$^+$)	this study
JE6274	DH5α/pPRP112 (P_{araBAD}, *prpE*-K248E, *bla*$^+$)	this study
JE6275	DH5α/pPRP113 (P_{araBAD}, *prpE*-G249A, *bla*$^+$)	this study
JE6276	DH5α/pPRP114 (P_{araBAD}, *prpE*$^+$, *bla*$^+$)	this study
JE6277	DH5α/pPRP115 (P_{araBAD}, *prpE*-K592A, *bla*$^+$)	this study
JE6278	DH5α/pPRP116 (P_{araBAD}, *prpE*-K592E, *bla*$^+$)	this study
	S. typhimurium	
JR501	*hsdSA29 hsdSB121 hsdL6 metA22 metE551 trpC2 ilv-452 rpsL120 xyl-404 galE719 H1-b H2-en,n,x* (Fels2$^-$) *fla-66 nml*$^-$	*49*
TR6583	*metE205 ara-9*	K. Sanderson via J. Roth
JE4313	*metE205 ara-9 prpE213*::*kan*$^+$ DEL*1231* (*acs*)	*3*

primers were used: P247A (plasmid pPRP87), 5′-CCGCCGACGTCGCGCTGGACGCCTTTCGCTTTG-3′; K248A (plasmid pPRP88), 5′-CCGCCGACGTCGCGCTGGACGCCGGCCGGTTTG-3′; K248E (plasmid pPRP90), 5′-CCGCCGACGTCGCGCTGGACGCCTTCCGGTTTG-3′; G249A (plasmid pPRP89), 5′-CCGCCGACGTCGCGCTGGACGGCTTTC-3′.

Plasmids pPRP100 and pPRP101. Site-directed mutations at K592 were constructed using three-primer PCR as described (*26*). The outer primers were a 5′ T7 promoter primer (5′-CGAAATTAATACGACTCACTAT-3′) and a 3′ reverse primer (5′-CATGACCTTATTACCAACCTC-3′), and the internal phosphorylated primers were K592A (5′-CGTTCCGGAGCGATGCTTCGC-3′) and K592E (5′-CGTTCCGGAGAGATGCTTCGC-3′). The 2.1-kb PCR products were identified by gel electrophoresis, excised from the gel, and purified using the QIAquick Gel Extraction kit (Qiagen, Chatsworth, CA). The purified PCR fragment was cloned by A-tailing the DNA and ligating into pGEM-T Easy Vector system (Promega, Madison, WI) according to manufacturer's instructions. The resulting plasmid was 5.1 kb (*bla*$^+$, Ap^r) and was called pPRP98 (*prpE*K592A) or pPRP99 (*prpE*K-592E). The *prpE* gene with site-directed mutations was removed from these plasmids with *Xba*I and *Kpn*I and cloned into pTYB2 digested with the same enzymes. The size of the final plasmids was 9.4 kb (*bla*$^+$, Ap^r), and were named pPRP100 (*prpE*K592A) or pPRP101 (*prpE*K592E). These plasmids were used for the overexpression and purification of PrpEK592A and PrpEK592E mutant proteins.

Plasmids pPRP109−113. Site-directed mutations in plasmids pPRP69, pPRP87−90 were moved onto plasmid pPRP54 using *Aat*II and *Sal*I restriction enzymes. These two restriction enzymes removed a 0.6-kb piece of *prpE* in pPRP54, which was replaced with the corresponding fragments from plasmids pPRP69 and pPRP87−90. The final plasmids were 8.0 kb (*bla*$^+$, Ap^r), and were called pPRP109, *prpE*G245A; pPRP110, *prpE*P247A; pPRP111, *prpE*K248A; pPRP112, *prpE*K248E; pPRP113, *prpE*G249A.

Plasmid pPRP114. The *prpE* gene was PCR amplified from strain TR6583 as described (*25*). The 5′ primer contained a *Kpn*I site (5′-AAAGGTACCGGCGTAAGTTCAACAGGAGAG-3′), the 3′ primer contained a *Xba*I site (5′-AAAGGGTCTAGACGCTGAGTCTAACCCGTT-3′). The PCR product was purified and cloned into pGEM-T as described above. The resulting plasmid was 4.9 kb (*bla*$^+$, Ap^r) and was called pPRP103. Plasmid pPRP103 was digested with *Kpn*I and *Xba*I to remove the *prpE* gene as a 1.9-kb fragment, which was cloned into pBAD30 cut with the same enzymes (*27*). The resulting plasmid was a *prpE* minimal gene clone, and the plasmid was 6.9 kb (*bla*$^+$, Ap^r) and was called pPRP108. During initial studies with pPRP108, this plasmid overproduced PrpE protein and was deleterious to growth of *S. enterica* (data not shown). To address these concerns, the DNA sequence upstream of *prpE* in plasmid pPRP54 was moved to pPRP108, which reduced the production of PrpE protein and allowed complementation of a *prpE* mutant (strain JE4313). This new plasmid was constructed by removing a 0.8-kb fragment from plasmid pPRP108 with

*Kpn*I and *Aat*II and replacing it with a 0.96-kb fragment from plasmid pPRP54 cut with the same enzymes. The final plasmid was 7.1 kb (*bla*$^+$, Ap^r), and was called pPRP114. The only difference between pPRP108 and pPRP114 is addition of approximately 160 bp to pPRP114, between the P_{araBAD} promoter and the *prpE* ribosome binding site. This 160 bp contains *prpD* 3′ sequence and intergenic sequence from the *S. enterica* chromosome (*1*). When comparing *prpE* complementing plasmids pPRP114 and pPRP54, it should be noted that pPRP54 also contains *S. enterica* chromosomal sequence downstream of *prpE* (*3*).

Plasmids pPRP115 and pPRP116. For construction of complementing plasmids of the *prpE*K592 mutations, three-primer PCR was performed as described above. The 5′-*Kpn*I, 3′-*Xba*I, and the internal K592A and K592E primers described above were used for PCR. The 1.9-kb PCR products were purified and cloned into pGEM-T as described above. The resulting plasmids were 4.9 kb (*bla*$^+$, Ap^r), and were called pPRP104 (*prpE*K592A) or pPRP105 (*prpE*K-592E). The *prpE* gene with site-directed mutations was removed from these plasmids with *Kpn*I and *Xba*I and cloned into plasmid pBAD30 digested with the same enzymes (*27*). The size of the resulting plasmids was 6.8 kb (*bla*$^+$, Ap^r), and were named pPRP106 (*prpE*K592A) or pPRP107 (*prpE*K592E). These plasmids did not complement a *prpE* mutant (data not shown). To address the concern that the PrpE mutant proteins were being overproduced, the region upstream of *prpE* in the *prpE*K592 alleles (pPRP106−107) was replaced with a fragment from pPRP54 as described above. The final plasmids were 7.1 kb (*bla*$^+$, Ap^r), and were called pPRP115 (*prpE*K592A) or pPRP116 (*prpE*K592E). These plasmids should be compared to control plasmid pPRP114, which was constructed in the same manner (see above).

Purification of Wild-Type and Mutant PrpE Proteins. Chitin Affinity Chromatography. Wild-type and mutant PrpE proteins were purified by chitin affinity chromatography as described (*20*). For efficient intein cleavage on the chitin resin, an additional glycine residue was added to the C-terminus of all PrpE proteins.

Enzyme Assays. Acyl-CoA Synthetase Assays. The acyl-CoA synthetase assay used was based on the coupled assay reported by Williamson (*28*). Standard acyl-CoA synthetase assays (1.0 mL) contained 50 mM HEPES buffer, pH 7.5, 3.0 mM PEP, 10 units MK, 10 units PK, 10 units LDH, 5 mM $MgCl_2$, 2.5 mM ATP, and 1.0 mM CoA. Acyl substrates were added at the following concentrations: β-alanine, 20 mM; D-alanine, 20 mM; L-alanine, 20 mM; glycine, 20 mM; sodium glyoxylate, 20 mM; sodium malonate, 20 mM; sodium mercaptoacetate, 20 mM; sodium propionate, 0.15 mM. For these assays, buffer and reagents were preincubated in quartz cuvettes at 37 °C in a Lambda Bio-40 spectrophotometer (Perkin-Elmer) equipped with a circulating water-jacket. After 3 min, assays were started with the addition of PrpE protein (0.25−1.0 μg), and the reaction was monitored for 10 min at 340 nm. Specific activities were calculated from the extinction coefficient of 12440 M^{-1} cm^{-1} for the oxidation of two molecules of NADH for each AMP released, and they are reported as mmol min^{-1} (mg of protein)$^{-1}$. Wild-type and mutant PrpE proteins were diluted in 50 mM HEPES, pH 7.5, with 1 mM TCEP prior to assay measurement. Using this assay, background levels of approximately 0.1−0.2 nmol/min were observed, and any acyl-CoA synthetase assays in this range were considered not detectable.

ATP Formation Assays. The ATP assay used was based on the one previously described (*4*, *28*). The reaction mixtures (1.0 mL) contained 50 mM HEPES buffer, pH 7.5, 3.0 mM D-glucose, 10 units HK, 10 units G6PDH, 5 mM $MgCl_2$, 2.5 mM sodium pyrophosphate, and 0.25 mg of PrpE protein. For these assays, buffer and reagents were preincubated in quartz cuvettes at 37 °C in a Lambda Bio-40 spectrophotometer. After 3 min, assays were started with propionyl-AMP, and the reaction was monitored for 10 min at 340 nm. Specific activities were calculated from the extinction coefficient of 6220 M^{-1} cm^{-1} for the reduction of one molecule of NAD for each ATP released, and they are reported as mmol min^{-1} (mg of protein)$^{-1}$. Significant background activity was not observed using this assay.

Determination of K_m and k_{cat} Values. Apparent K_m values were determined for PrpE substrates by varying one substrate at a fixed concentration of the other two substrates. Initial velocities of the acyl-CoA synthetase activity (with 2.5 mM ATP, 5 mM $MgCl_2$, and 1 mM CoA) were determined as a function of propionate concentration (7.5−2000 μM), acetate concentration (0.05−20 mM), and butyrate concentration (1−60 mM). Initial velocities of the propionyl-CoA synthetase activity (with 2 mM propionate and 5 mM $MgCl_2$) were determined as a function of ATP concentration (25−2500 μM) and CoA concentration (25−1000 μM). Acyl-CoA synthetases assays were performed as described above. Initial velocities of the ATP formation assays (with 5 mM $MgCl_2$) were determined as a function of propionyl-AMP concentration (4.4−154 μM) and pyrophosphate concentration (25−2500 μM). ATP formation assays were performed as described above. Assay sets contained 10−12 points, and each set was performed at least three times. Initial velocity data were analyzed using the program GraFit 4.0 (*29*).

Determination of K_i Values. Inhibition of the PrpE propionyl-CoA synthetase reaction was performed with adenosine 5′-propyl phosphate (propyl-AMP). Assays were performed varying both substrate and inhibitor at five different concentrations (25 assays). Concentrations of substrates used: (i) ATP inhibition, ATP (50−250 μM), and propyl-AMP (0.0125 to 0.05 μM); (ii) propionate inhibition, propionate (20−100 μM), and propyl-AMP (0.25 to 1.0 μM); (iii) CoA inhibition, CoA (100−400 μM), and propyl-AMP (0.5−2.0 μM); (iv) propionyl-AMP inhibition, propionyl-AMP (20−100 μM), and propyl-AMP (0.025 to 0.10 μM). Each set of assays was performed at least three times. Initial velocity data were analyzed using the program GraFit 4.0, and K_i values were determined by fitting velocity data into the appropriate rate equations in Grafit 4.0 (*29*).

Chemical Synthesis. Propionyl-AMP. The synthesis of propionyl-AMP was performed as described (*5*). The compound was approximately 93% pure as determined by HPLC (protocol described below) with the primary contaminant being AMP. The UV−visible spectrum of propionyl-AMP was similar to the one for AMP. The mass of the compound was verified using negative ion ESI-MS. The mass observed, $m/z = 402$, correlated to the negative ion of the expected mass of 403 Da.

Propyl-AMP. The synthesis of propyl-AMP was performed as described (*30*). The compound was purified on DEAE-

Sephadex A-25 as described by Yasuda and Inoue (*31*), except an ammonium acetate gradient was used instead of NH_4HCO_3. A mass of $m/z = 388$ was observed in negative ion ESI-MS, correlated with that of the negative ion of the expected mass of 389 Da.

HPLC of PrpE Reactions. Equipment and Solvents. Samples were run on Waters 600 solvent delivery system equipped with a Waters 900 PDA detector. A LUNA 5μ C18 column (150 × 4.6 mm, 5 μM particle diameter, Phenomenex, Torrance, CA) was used for all separations, and flow-rate was maintained at 1 mL/min. The separations were monitored at 260 nM. The solvent system was based on one previously described (*32*). The following solvents were prepared: solvent A: 100 mM KH_2PO_4 with 2 mM TBAB; solvent B: 100 mM KH_2PO_4 with 2 mM TBAB and 15% CH_3CN; solvent C: 100 mM KH_2PO_4 with 2 mM TBAB and 35% CH_3CN. All solvents were adjusted to pH 3.3 with H_3PO_4.

Conversion of Propionyl-AMP to ATP. A 0.1-mL reaction mixture was prepared with the following components: 50 mM HEPES buffer at pH 7.5, 2 mM propionyl-AMP, 2 mM sodium pyrophosphate, 5 mM $MgCl_2$, and 5 μg of PrpE protein. The reaction was incubated for 60 min at 37 °C and was stopped with 1 μL of hydrochloric acid. The reaction was kept on ice and 10 μL was analyzed by RP-HPLC. The sample was separated using the following conditions: 10 min linear gradient of 100% solvent A to 100% solvent B, followed by 10 min isocratic of 100% solvent B. Standards eluted with the following retention times: AMP, 9.0 min; propionyl-AMP, 15.5 min; ATP, 16.8 min.

Conversion of Propionyl-AMP to Propionyl-CoA. A 0.1-mL reaction mixture was prepared with the following components: 50 mM HEPES buffer at pH 7.5, 2 mM propionyl-AMP, 2 mM CoA, and 5 μg of PrpE protein. The reaction was stopped and injected onto the C_{18} column as described above. The sample was separated using the following conditions: 5 min isocratic elution using 100% solvent B, 10 min linear gradient to 100% solvent C, and 5 min isocratic elution using 100% solvent C. Standards eluted with the following retention times: AMP, 1.9 min; propionyl-AMP, 3.4 min; CoA, wide peak at 11.5−13 min; propionyl-CoA, 17.2 min.

^{31}P NMR Spectroscopy. Peak assignments were based on experiments with known standards. The ^{31}P NMR spectra are available upon request.

In Vitro Synthesis of Propionyl-CoA. The following were combined in a 0.5-mL reaction mixture: 50 mM potassium phosphate buffer at pH 7.5, 5 mM sodium propionate, 5 mM ATP, 5 mM CoA, 10 mM $MgCl_2$, and 30 μg of PrpE protein. The reaction was incubated for 60 min at 37 °C. CoA solutions were prepared fresh for each experiment.

In Vitro Conversion of Propionyl-AMP to ATP. The following were combined in a 0.5-mL reaction mixture: 50 mM phosphate buffer at pH 7.5, 5 mM propionyl-AMP, 5 mM PPi, 10 mM $MgCl_2$, and 30 μg of PrpE protein. The reaction was incubated for 60 min at 37 °C.

In Vitro Conversion of Propionyl-AMP to Propionyl-CoA. The following were combined in a 0.5-mL reaction mixture: 50 mM potassium phosphate buffer at pH 7.5, 2 mM propionyl-AMP, 2 mM CoA, and 5 μg of PrpE protein. The reaction was incubated for 60 min at 37 °C.

Preparation of Samples for ^{31}P NMR. Each mixture was transferred into a NMR tube (5 mm, Wilmad Glass, Buena, NJ), and 0.1 mL of 100% D_2O was added. D_2O and TMS were purchased from Cambridge Isotope Labs (Andover, MA).

^{31}P NMR Spectra Acquisition. ^{31}P NMR spectra were acquired at 161.98 MHz with a deuterium lock on a Bruker Instruments DMX-400 Avance console with a 9.4 T wide-bore magnet (Nuclear Magnetic Resonance Facility at the University of Wisconsin-Madison). Spectra were Fourier transformed with 3 Hz line-broadening. Chemical shifts presented in this work were relative to H_3PO_4 which was set to 0.0 ppm.

Other Procedures. Protein concentrations were determined by the method of Bradford (*33*) using the BioRad protein reagent (BioRad, Hercules, CA). A standard curve was generated for protein determinations with bovine serum albumin. Proteins were separated by SDS−PAGE (*34*) using 12% polyacrylamide gels and were visualized with Coomassie Blue (*35*). Midrange standards (14−150 kDa) were used for SDS−PAGE (Novagen). All UV−vis spectroscopy was performed on a computer-controlled Lambda Bio-40 spectrophotometer (Perkin-Elmer) equipped with temperature control.

RESULTS

PrpE Purification and Identification of Reaction Byproducts. PrpE protein was purified to homogeneity using chitin affinity chromatography followed by intein cleavage. The resulting PrpE protein contained one additional C-terminal glycine. The addition of this G residue was needed to optimize intein cleavage (*20*). The specific activity of the PrpE protein was 22 μmol min^{-1} mg^{-1}, which compared favorably to other acyl-CoA synthetases (*36*−*38*).

Propionyl-CoA was previously identified as the end-product of the reaction (*3*), but the reaction byproducts were not determined. To identify these byproducts, PrpE reactions were analyzed by ^{31}P NMR spectroscopy. AMP and pyrophosphate were observed in the ^{31}P NMR spectrum following the incubation of propionate, Mg-ATP, CoA, and PrpE in a reaction mixture (data not shown). This result supported the proposal that PrpE proceeded via a propionyl-AMP intermediate (*3*).

Propionyl-AMP is a Substrate for PrpE. To test whether propionyl-AMP was a substrate for the PrpE enzyme, this compound was chemically synthesized. The PrpE enzyme was incubated with propionyl-AMP and Mg-pyrophosphate and the formation of ATP was monitored by HPLC (data not shown). The addition of PrpE to the reaction mixture converted the propionyl-AMP and pyrophosphate to ATP and AMP. ^{31}P NMR was used to monitor the fate of pyrophosphate during the course of the reaction. Pyrophosphate levels dropped following the addition of PrpE protein to the reaction mixture (data not shown). Although the formation of propionate was not observed, this byproduct was expected upon cleavage of propionyl-AMP (*5*). The synthesis of propionyl-CoA from propionyl-AMP and CoA was also monitored by HPLC (data not shown). The addition of PrpE to a reaction mixture containing propionyl-AMP and CoA resulted in the formation of propionyl-CoA and AMP. This reaction did not require divalent cations as previously

Table 2: Kinetic Parameters of PrpE

substrate	K_m (μM)	k_{cat} (s^{-1})	k_{cat}/K_m (mM^{-1} s^{-1})
propionate	20 ± 2	33 ± 2	1644
acrylate	279 ± 14	26 ± 1	92
acetate	1700 ± 145	32 ± 1	19
butyrate	5600 ± 210	6 ± 0.2	1
ATP	57 ± 5	34 ± 1	600
CoA	215 ± 31	42 ± 1	196
PPi	254 ± 9	79 ± 5	310
propionyl-AMP	23 ± 2	78 ± 4	3440

observed for other acyl-CoA synthetases (*5*). The specific activity of PrpE in both half-reactions was also measured using propionyl-AMP as substrate (Table 2). PrpE protein synthesized ATP from propionyl-AMP and Mg-pyrophosphate at 66 μmol min^{-1} mg^{-1}, and the enzyme converted propionyl-AMP to propionyl-CoA at 32 μmol min^{-1} mg^{-1}. Both of these half-reactions were faster than the overall reaction, which was 22 μmol min^{-1} mg^{-1}. The results of these experiments demonstrated that propionyl-AMP was a substrate for the PrpE enzyme.

Kinetic Parameters. Using a continuous spectrophotometric assay to detect AMP levels (*28*), the kinetic parameters of the PrpE protein for ATP, CoA, acyl substrates, and reaction intermediates were determined (Table 2).

Acyl Substrates. Propionate was the preferred acyl substrate with a K_m of 20 μM. Acrylate was the next best acyl substrate with a K_m of 280 μM, although the k_{cat}/K_m is more than 17-fold lower than propionate. Acetate was also a substrate for PrpE, but the affinity of the enzyme for acetate was significantly lower (K_m of 1.7 mM). The k_{cat}/K_m for acetate was more than 86-fold lower than propionate. Butyrate was a very poor substrate for PrpE with a K_m of 5.6 mM and a k_{cat}/K_m 1640-fold lower than propionate. Recently, *S. enterica* PrpE was also purified by Valentin et al. (*8*), and K_m values of 50 μM for propionate and 0.9 mM for acetate were reported are in agreement with those reported in this work.

Other acyl compounds not shown in Table 2 were also tested as substrates for PrpE. Mercaptoacetoacetate was a good substrate for PrpE at a specific activity of 18 μmol min^{-1} mg^{-1}. Glyoxylate and glycine were poor substrates at specific activities of 0.65 and 0.060 μmol min^{-1} mg^{-1}, respectively. β-Alanine, L-alanine, D-alanine, and malonate were not substrates for the enzyme.

ATP and Coenzyme A. The kinetic parameters for other PrpE substrates were also determined (Table 2). K_m values for Mg-ATP and CoA were 57 and 215 μM, respectively, which compare favorably to those reported for other acyl-CoA synthetases (*36*−*38*). The K_m values for reaction intermediates were determined using hexokinase and glucose-6-phosphate dehydrogenase (*5*), and the results were 254 μM for Mg−PPi and 23 μM for propionyl-AMP.

Inhibition Kinetics. Adenosine 5′-alkyl phosphates are known inhibitors of acyl-CoA synthetases (*39*). To investigate the PrpE reaction mechanism, adenosine 5′-propyl phosphate (propyl-AMP) was synthesized and tested against PrpE substrates (see Experimental Procedures). As shown in Figure 3A and B, propyl-AMP showed competitive inhibition against ATP (K_i = 18 nM) and mixed-inhibition against propionate (K_i = 343 nM). These results were consistent with those reported in the original study of these inhibitors (*39*). As shown in Figure 3C and D, propyl-AMP showed uncompetitive inhibition against CoA (K_i = 1260 nM) and competitive inhibition versus the reaction intermediate propionyl-AMP (K_i = 34 nM). These results strongly suggested a Bi Uni Uni Bi Ping Pong kinetic mechanism for the reaction catalyzed by the PrpE enzyme (*40*). The kinetic mechanisms of several acyl-CoA synthetases have been determined, and all show ordered Ping Pong mechanisms (*36*, *38*, *41*). Although full ter-reactant kinetics was not performed, it is unlikely that the PrpE reaction will proceed via a different kinetic mechanism.

Residues Involved in Propionyl-AMP Synthesis. Previous studies on motif 1 with other acyl-CoA synthetases suggested that these residues were important for adenylate formation (*15*, *17*, *18*, *36*, *38*). Although studies on this motif have identified residues that affect catalytic activities, many of these mutant proteins had only small decreases in k_{cat} or specific activity as compared to their respective wild-type proteins (*15*, *17*, *36*, *38*). Mutations in motif 1 of 4-CBA-CoA synthetase identified residues that reduced the turnover rate 1000- to 5000-fold (*17*). This study prompted initial experiments with motif 1 in PrpE presented in this report. Using synthetic propionyl-AMP, the adenylation reaction of PrpE mutant proteins could be bypassed to identify residues critical for this half-reaction. For these experiments, conserved residues G245, P247, K248, and G249 were all changed to alanines, with an additional change of residue K248 to glutamate. These mutations were introduced into *prpE* carried on plasmid pPRP68, and the site-directed mutant proteins were overproduced and purified using chitin-affinity chromatography (see Experimental Procedures).

The specific activity of each mutant PrpE protein was determined for the complete reaction and for the conversion of propionyl-AMP and pyrophosphate to ATP and propionate, and for the conversion of propionyl-AMP and CoA to propionyl-CoA and AMP. As shown in Table 3, the *prpE*G245A and *prpE*P247A mutations had little effect on the activity of the enzyme. The specific activity of the PrpEG245A mutant protein was reduced 27−70% in the three types of reactions, while the PrpEP247A mutant protein was only reduced 5−17%. However, the PrpEK248A and PrpEG249A mutant proteins showed a 73−90% drop in specific activity during the conversion of propionate to propionyl-CoA and for the conversion of propionyl-AMP to propionate, and a 97% drop in specific activity in the reaction that synthesized ATP from propionyl-AMP and PPi. The *prpE*K248E mutation had the most pronounced negative effect (95−96% drop) on the specific activity in both the complete reaction and in the conversion of propionyl-AMP to propionyl-CoA, and a 98.5% drop in the specific activity during the conversion of propionyl-AMP and pyrophosphate to ATP and propionate.

Effect of the Mutations at Residue K592. During the course of this work, residue K529 of firefly luciferase was identified as a key residue for the adenylation reaction (*19*). This study suggested the corresponding residue of PrpE, K592, could also be critical for propionyl-AMP synthesis. Site-directed *prpE* alleles *prpE*K592A and *prpE*K592E were constructed, and the resulting mutant proteins were purified.

As shown in Table 3, PrpEK592A and PrpEK592E mutant proteins were unable to catalyze the conversion of propionate

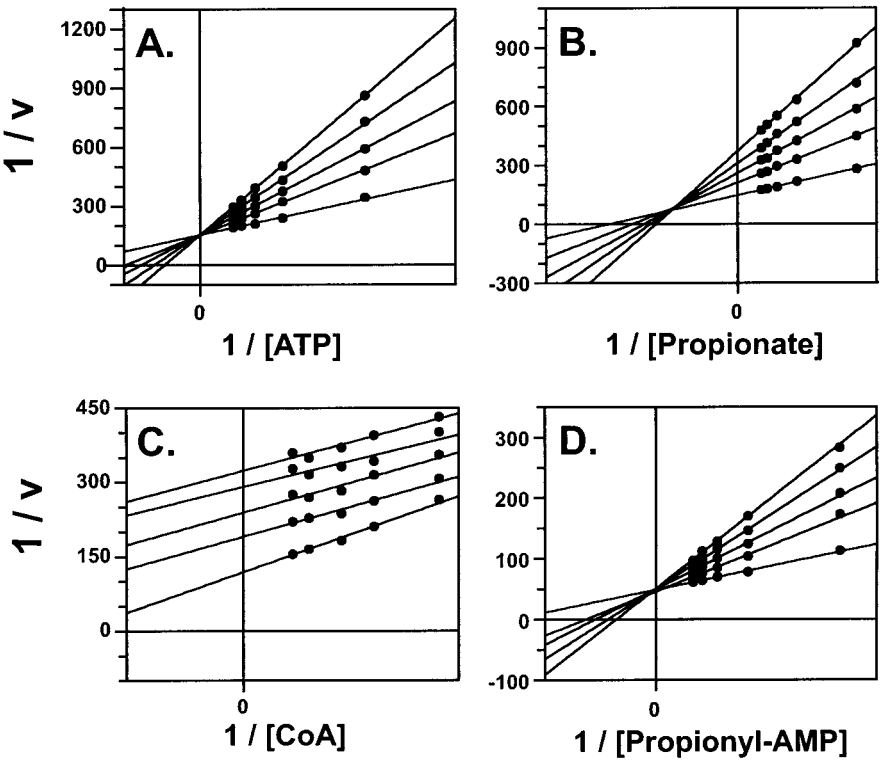

FIGURE 3: PrpE inhibition kinetics using propyl-AMP. (A) competitive versus ATP; (B) mixed-inhibition versus propionate; (C) uncompetitive versus CoA; and (D) competitive versus propionyl-AMP.

Table 3: Specific Activities of PrpE Site-Directed Mutants

	complete reaction[a]		ATP synthesis[a]		propionyl-CoA synthesis[b]	
allele	specific act	% wild-type	specific act	% wild-type	specific act	% wild-type
wild-type	22 (± 0.6)	100	66 (± 6)	100	31 (± 2)	100
G245A	13 (± 0.15)	58	48 (± 3)	73	9 (± 1)	29
P247A	21 (± 0.5)	95	67 (± 2)	101	26 (± 3)	84
K248A	3 (± 0.1)	12	2 (± 0.06)	2.4	3 (± 0.2)	10
K248E	1 (± 0.002)	5.8	1 (± 0.03)	1.5	1 (± 0.1)	3
G249A	2 (± 0.2)	11	2 (± 0.2)	3.2	8 (± 0.3)	26
K592A	ND[c]		1 (± 0.05)	1.2	50 (± 6)	161
K592E	ND		0.004 (± 0.001)	0.007	14 (± 0.5)	45

[a] The average of three independent determinations. [b] The average of six independent determinations. [c] ND, not detectable under the assay conditions used.

to propionyl-CoA. If these mutant proteins could perform the propionyl-CoA synthetase reaction, it was below the limit of detection of the assay (see Experimental Procedures). Surprisingly, the PrpEK592A mutant enzyme was able to convert propionyl-AMP and pyrophosphate to ATP and propionate, although at a 82-fold lower specific activity than the wild-type enzyme. In contrast, the specific activity of the PrpEK592E mutant enzyme for this reaction was reduced over 15000-fold. A similar fold reduction in the propionyl-CoA synthetase assay would have been at the limit of detection, suggesting the interconversion of propionate and propionyl-AMP by the PrpEK592E mutant was nearly undetectable. Both mutant enzymes were effective for conversion of propionyl-AMP to propionyl-CoA; compared to wild-type PrpE enzyme the conversion rates were 174 and 44% for the PrpEK592A and PrpEK592E mutant enzymes, respectively. For the PrpEK592A mutant protein, the conversion of propionyl-AMP to propionyl-CoA was inhibited by ATP. At ATP levels of 1 mM, the specific activity of the mutant protein dropped 60% (data not shown). Interestingly, the PrpEK592E mutant protein was not inhibited by ATP in the reaction mixture. These results demonstrated that residue K592 of PrpE plays an important role in the adenylation reaction. The negative effect of ATP requires further analysis.

Effect of PrpE Motif 1 Site-Directed Mutations on the Activity of Proteins in Vivo. During growth of *S. enterica* on propionate, PrpE and acetyl-CoA synthetase (encoded by *acs*) can activate propionate to propionyl-CoA to initiate the 2-methylcitric acid cycle (*3*). The requirement for the PrpE enzyme in propionate catabolism was addressed using a *prpE acs* double mutant strain (JE4313). Plasmid pPRP54 (P_{araBAD}-*prpE*$^+$) carried the *prpE*$^+$ allele under control of the L-arabinose inducible P_{araBAD} promoter, which was needed to test the function of *prpE* alleles in vivo (*3*). All motif 1 site-directed *prpE* alleles were constructed on plasmid pPRP54 using unique *Sal*I and *Aat*II sites flanking the motif (see Experimental Procedures). Strain JE4313 was transformed with these plasmids and control plasmids (pPRP54 and pBAD30), and the resulting strains were tested for growth on minimal media containing propionate as the source of carbon and energy. As shown in Table 4, the *prpE*$^+$ control (plasmid pPRP54) restored growth of strain JE4313 on propionate when 100 μM arabinose was present in the medium. The doubling time of this strain was the same as strain TR6583, which has a wild-type *prpRBCDE*$^+$ operon in its genome. All motif 1 *prpE* mutant alleles compensated for the lack of PrpE function at 100 μM arabinose. The PrpEK248E and PrpEG249A mutant proteins, which displayed the lowest specific activities in vitro, also supported growth of strain JE4313 on propionate. The control plasmid carrying the wild-type *prpE*$^+$ allele, restored growth of strain

Table 4: In Vivo Function of PrpE Mutant Proteins

line	chromosome	plasmid	site-directed mutat	doubling times (h)[a] no arabinose	25 μM arabinose	100 μM arabinose
1	*prpE*$^+$ *acs*$^+$	pBAD30	VOC[b]	6 (± 0.5)	6 (± 1)	6 (± 0.5)
2	*prpE*$^-$ *acs*$^-$	pBAD30	VOC	>60	>60	>60
3	*prpE*$^-$ *acs*$^-$	pPRP54	none[c]	22 (± 2)	9 (± 1)	6 (± 0.5)
4	*prpE*$^-$ *acs*$^-$	pPRP109	G245A	29 (± 3)	12 (± 1)	6.5 (± 1)
5	*prpE*$^-$ *acs*$^-$	pPRP110	P247A	24 (± 3)	10 (± 1)	6 (± 1)
6	*prpE*$^-$ *acs*$^-$	pPRP111	K248A	38.5 (± 3)	18.5 (± 2.5)	7 (± 0.5)
7	*prpE*$^-$ *acs*$^-$	pPRP112	K248E	48 (± 12)	30 (± 9)	11.5 (± 1)
8	*prpE*$^-$ *acs*$^-$	pPRP113	G249A	57 (± 27)	30 (± 9)	10 (± 0.5)
9	*prpE*$^-$ *acs*$^-$	pPRP114	none	33 (± 3)	NT[d]	9 (± 2)[e]
10	*prpE*$^-$ *acs*$^-$	pPRP115	K592A	NG[f]	NT	NG
11	*prpE*$^-$ *acs*$^-$	pPRP116	K592E	NG	NT	NG

[a] Error reported as standard deviation. [b] VOC, vector-only control. [c] None, wild-type *prpE* plasmid. [d] NT, not tested. [e] When 250 μM arabinose was included in the medium, the doubling time was reduced to 6 h. This concentration of arabinose did not reduce the doubling time of the strain in line 3 any further. [f] NG, no growth.

JE4313 with as low as 25 μM arabinose in the medium, although the doubling time was relatively long, i.e., 9 h. This concentration of arabinose (25 μM), however, was useful for assaying the efficiencies of the site-directed mutant proteins to support growth on propionate in vivo. Strain JE4313 carrying a plasmid encoding the P247A or G245A mutant protein grew almost identically to the *prpE*$^+$ control strain at 25 μM arabinose; the doubling times for the strain carrying the *prpE*G245A allele was approximately 30% higher, and the strain carrying the *prpE*P247A allele was only 10% higher. Plasmids containing the *prpE*K248A, *prpE*K248E, and *prpE*G249A alleles also complemented at this level of induction, although the doubling times of the *prpE*K248E and *prpE*G249A alleles were 3-fold higher than the *prpE*$^+$ control (Table 4, line 7 or 8 vs line 3). The doubling time of the strain carrying the *prpE*K248A allele was 20 h, only 2-fold higher than the control strain (Table 4, line 3 vs line 6).

In Vivo Assessment of the Importance of Residue K592. The effect of mutations in residue K592 was also tested in vivo using strain JE4313. Arabinose-inducible plasmids containing the *prpE*K592A or *prpE*K592E alleles were constructed using plasmid pBAD30 (see Experimental Procedures). The resulting plasmids containing the *prpE*K592 alleles (pPRP115 and pPRP116) were identical to the pPRP54-based plasmids described above, except that they lacked *S. enterica* sequence downstream of *prpE* (*1*, *3*). A control plasmid (pPRP114) was constructed in the same manner, which verified the absence of this downstream sequence had only a small effect on complementation (Table 4, line 3 vs line 9). Both plasmids containing *prpE*K592 alleles (pPRP115 and pPRP116) failed to support growth of strain JE4313 on propionate (Table 4, lines 10 and 11), even at arabinose levels >100 μM (data not shown).

DISCUSSION

In this report, the propionyl-CoA synthetase of *S. enterica*, encoded by *prpE*, was purified and kinetically characterized. The role of conserved residues in propionyl-AMP formation was addressed, and the importance of these residues during growth of *S. enterica* on propionate was tested.

The prpE Gene Encodes a Bona Fide, Highly Specific Propionyl-CoA Synthetase Enzyme. The results reported here demonstrate that the PrpE protein has all the properties of acyl-CoA synthetase. Noteworthy, however, is the high specificity of PrpE for propionate. Acyl chain-length was very important to the enzyme considering that acetate and butyrate were poor substrates. Interestingly, PrpE can substitute for acetyl-CoA synthetase in *S. enterica* (*3*), suggesting that low levels of this activity are sufficient to support growth on acetate. We previously reported that butyrate was not a substrate for PrpE (*3*). Using an assay with increased sensitivity, it became clear that butyrate was a substrate for the PrpE enzyme, albeit a poor one. The affinity of the enzyme for butyrate was poor (K_m = 5.6 mM), and the enzyme turned over slowly (k_{cat} = 6 s^{-1}) when butyrate was the substrate. The acyl substrate specificities of PrpE make this enzyme an ideal candidate for applications requiring the synthesis of propionyl-CoA in the presence of other acyl groups.

Motif 1 Is Important for Adenylation. Results of the mutational analysis of motif 1, clearly showed that residues K248 and G249 were important for adenylation. Noteworthy were the minor effects the G245A and P247A mutations had on the specific activities of the enzyme. Mutations of the corresponding residues in 4-CBA synthetase (i.e., G166I and P168A) reduced k_{cat} 14- and 5000-fold, respectively (*17*), although the G245A mutation in PrpE is more conservative than the G166I mutation of 4-CBA synthetase.

The in vitro results suggested the K248 and G249 residues were important for function. However, the PrpE mutant enzymes were only 88−94% slower than the wild-type enzyme in the complete reaction. Complementation experiments of a *S. enterica prpE acs* double mutant strain (JE4313) showed that PrpE mutant proteins (including those carrying mutations in residues K248 or G249) were functional and supported growth of the cell on propionate as the sole source of carbon and energy. Strains carrying plasmids encoding the PrpEK248A, PrpEK248E, or PrpEG249A mutant proteins had the longest doubling times, however, a result consistent with the reduced catalytic activities displayed by these mutant enzymes in vitro.

Residue K592 Is Required for Propionyl-AMP Synthesis. Potential Practical Use of the PrpEK592 Mutant Protein. The PrpEK592A and PrpEK592E mutant proteins showed no propionyl-CoA synthetase activity in vitro, but effectively catalyzed the conversion of propionyl-AMP to propionyl-CoA. The deficiencies in these mutant enzymes appeared to be in adenylation reaction, although the PrpEK592A mutant could convert propionyl-AMP to propionate and ATP at a slow rate. It is possible the propionyl-CoA synthetase activity of the PrpEK592A mutant was not observed due to ATP inhibition, a property of this mutant protein that requires further investigation. Taken together, these observations suggest that residue K592 is required for propionyl-AMP synthesis. These results support the observations made with the corresponding lysine mutant (K529) of luciferase (*19*), and they provide further evidence that acyl-CoA synthetases and luciferases share a similar enzyme mechanism. Consistent with these results, PrpEK592 mutant proteins failed to support growth of a *prpE acs* double mutant strain (JE4313) on propionate. Acyl-AMP pools have been reported to exist in procaryotes, and acyl-CoA synthetases are likely to be the only source of these pools (*42*, *43*). Acyl-CoA synthetases

with a mutation corresponding to the K592 residue would make useful biochemical tools for measuring acyl-AMP levels.

NOTE ADDED AFTER ASAP POSTING

An earlier version posted ASAP on 1/19/02 contained an incorrect propionyl-AMP concentration in the Experimental Section-Determination of K_m and k_{cat} values. It has now been corrected in this version posted 2/12/02.

ACKNOWLEDGMENT

NMR studies were carried out at the National Magnetic Resonance Facility at Madison with support from the NIH Biomedical Technology Program (RR02301) and additional equipment funding from the University of Wisconsin, NSF Academic Infrastructure Program (BIR-9214394), NIH Shared Instrumentation Program (RR02781, RR08438), NSF Biological Instrumentation Program (DMB-8415048), and U.S. Department of Agriculture.

REFERENCES

1. Horswill, A. R., and Escalante-Semerena, J. C. (1997) *J. Bacteriol. 179*, 928−940.
2. Horswill, A. R., and Escalante-Semerena, J. C. (1999) *J. Bacteriol. 181*, 5615−5623.
3. Horswill, A. R., and Escalante-Semerena, J. C. (1999) *Microbiology 145*, 1381−1388.
4. Berg, P. (1956) *J. Biol. Chem. 222*, 991−1013.
5. Berg, P. (1956) *J. Biol. Chem. 222*, 1015−1023.
6. Babbitt, P. C., and Kenyon, G. L. (1992) *Biochemistry 31*, 5594−5604.
7. Conti, E., Stachelhaus, T., Marahiel, M. A., and Brick, P. (1997) *EMBO J. 16*, 4174−4183.
8. Valentin, H. E., Mitsky, T. A., Mahadeo, D. A., Tran, M., and Gruys, K. J. (2000) *Appl. Environ. Microbiol. 66*, 5253−5258.
9. Pfeifer, B. A., Admiraal, S. J., Gramajo, H., Cane, D. E., and Khosla, C. (2001) *Science 291*, 1790−1792.
10. Pfeifer, B. A., and Khosla, C. (2001) *Microbiol. Mol. Biol. Rev. 65*, 106−118.
11. Stachelhaus, T., Mootz, H. D., and Marahiel, M. A. (1999) *Chem. Biol. 6*, 493−505.
12. Kricka, L. J. (2000) *Methods Enzymol. 305*, 333−345.
13. Lundin, A. (2000) *Methods Enzymol. 305*, 346−370.
14. Conti, E., Franks, N. P., and Brick, P. (1996) *Structure 4*, 287−298.
15. Gocht, M., and Marahiel, M. A. (1994) *J. Bacteriol. 176*, 2654−2662.
16. Dieckmann, R., Pavela-Vrancic, M., Pfeifer, E., Von Dhören, H., and Kleinkauf, H. (1997) *Eur. J. Biochem. 247*, 1074−1082.
17. Chang, K.-H., Xiang, H., and Duanaway-Mariano, D. (1997) *Biochemistry 36*, 15650−15659.
18. Jung, J. W., An, J. H., Na, K. B., Kim, Y. S., and Lee, W. (2000) *Protein Sci 9*, 1294−1303.
19. Branchini, B. R., Murtiashaw, M. H., Magyar, R. A., and Anderson, S. M. (2000) *Biochemistry 39*, 5433−5440.
20. Horswill, A. R., Dudding, A. R., and Escalante-Semerena, J. C. (2001) *J. Biol. Chem. 276*, 19094−19101.
21. Inoue, H., Nojima, H., and Okayama, H. (1990) *Gene 96*, 23−28.
22. Berkowitz, D., Hushon, J. M., Whitfield, H. J., Roth, J., and Ames, B. N. (1968) *J. Bacteriol. 96*, 215−220.
23. Balch, W. E., Fox, G. E., Magrum, L. J., Woese, C. R., and Wolfe, R. S. (1979) *Microbiol. Rev. 43*, 260−296.
24. Seidman, C. G., Struhl, K., Sheen, J., and Jessen, T. (1997) in *Current Protocols in Molecular Biology* (Ausubel, F. M., Brent, R., Kingston, R. E., Moore, D. D., Seidman, J. G., Smith, J. A., and Struhl, K., Eds.) pp 1.8−1.8.10, Wiley-Interscience, New York.
25. Horswill, A. R., and Escalante-Semerena, J. C. (2001) *Biochemistry 40*, 4703−4713.
26. Michael, S. F. (1994) *BioTechniques 16*, 410−414.
27. Guzman, L.-M., Belin, D., Carson, M. J., and Beckwith, J. (1995) *J. Bacteriol. 177*, 4121−4130.
28. Williamson, J. R., and Corkey, B. E. (1969) in *Methods in Enzymology* (Lowenstein, J. M., Ed.) pp 494−497, Academic Press, New York.
29. Leatherbarrow, R. J. (1998) *GraFit Version 4.0.*, Erithacus Software Ltd., Staines, UK.
30. Khorana, H. G. (1959) *J. Am. Chem. Soc. 81*, 4657−4660.
31. Yasuda, T., and Inoue, Y. (1983) *J. Biochem. (Tokyo) 94*, 1475−1481.
32. Kawamoto, Y., Shinozuka, K., Kunitomo, M., and Haginaka, J. (1998) *Anal. Biochem 262*, 33−38.
33. Bradford, M. M. (1976) *Anal. Biochem. 72*, 248−255.
34. Laemmli, U. K. (1970) *Nature 227*, 680−685.
35. Sasse, J. (1991) in *Current Protocols in Molecular Biology* (Ausubel, F. A., Brent, R., Kingston, R. E., Moore, D. D., Seidman, J. G., Smith, J. A., and Struhl, K., Eds.) pp 10.6.1−10.6.8, Wiley-Interscience, New York.
36. An, J. H., Lee, G. Y., Jung, J. W., Lee, W., and Kim, Y. S. (1999) *Biochem. J. 344*, 159−166.
37. Chang, K.-H., Liang, P.-H., Beck, W., Scholten, J. D., and Dunaway-Mariano, D. (1992) *Biochemistry 31*, 5605−5610.
38. Koo, H. M., and Kim, Y. S. (2000) *Arch. Biochem. Biophys. 378*, 167−174.
39. Grayson, N. A., and Westkaemper, R. B. (1988) *Life Sci. 43*, 437−444.
40. Fromm, H. J. (1967) *Biochim. Biophys. Acta 139*, 221−230.
41. Farrar, W. W., and Plowman, K. M. (1979) *Int. J. Biochem. 10*, 583−588.
42. Barak, R., Welch, M., Yanovsky, A., Oosawa, K., and Eisenbach, M. (1992) *Biochemistry 31*, 10099−11107.
43. Ramakrishnan, R., Schuster, M., and Bourret, R. B. (1998) *Proc. Natl. Acad. Sci. U.S.A. 95*, 4918−4923.
44. Blattner, F. R., Plunkett, G., III, Bloch, C. A., Perna, N. T., Burland, V., Riley, M., Collado-Vides, J., Glasner, J. D., Rode, C. K., Mayhew, G. F., Gregor, J., Davis, N. W., Kirkpatrick, H. A., Goeden, M. A., Rose, D. J., Mau, B., and Shao, Y. (1997) *Science 277*, 1453−1474.
45. An, J. H., and Kim, Y. S. (1998) *Eur. J. Biochem. 257*, 395−402.
46. Kratzschmar, J., Krause, M., and Marahiel, M. A. (1989) *J. Bacteriol. 171*, 5422−5429.
47. Mootz, H. D., and Marahiel, M. A. (1997) *J. Bacteriol. 179*, 6843−6850.
48. de Wet, J. R., Wood, K. V., DeLuca, M., Helinski, D. R., and Subramani, S. (1987) *Mol. Cell Biol. 7*, 725−737.

BI015647Q